

Ultrasound Viscosity Imaging in Breast Lesions: A Multicenter Prospective Study

WanRu Jia, MD¹, ShuJun Xia, MD¹, XiaoHong Jia, MD, BingHui Tang, ShuZhen Cheng, MeiYuan Nie, Ling Guan, Ying Duan, MengYan Zhang, Xia Chen, Hui Zhang, BaoYan Bai, HaiYun Jia, Ning Li, CongCong Yuan, MD, EnHeng Cai, MD, YiJie Dong, MD, JingWen Zhang, MD, Yi Jia, MD, Juan Liu, MD, ZhenYun Tang, MD, Ting Luo, MD, XiaoXiao Zhang, MD, WeiWei Zhan, MD, Ying Zhu, MD, JianQiao Zhou, MD

Rationale and Objectives: To explore and validate the clinical value of ultrasound (US) viscosity imaging in differentiating breast lesions by combining with BI-RADS, and then comparing the diagnostic performances with BI-RADS alone.

Materials and Methods: This multicenter, prospective study enrolled participants with breast lesions from June 2021 to November 2022. A development cohort (DC) and validation cohort (VC) were established. Using histological results as reference standard, the viscosity-related parameter with the highest area under the receiver operating curve (AUC) was selected as the optimal one. Then the original BI-RADS would upgrade or not based on the value of this parameter. Finally, the results were validated in the VC and total cohorts. In the DC, VC and total cohorts, all breast lesions were divided into the large lesion, small lesion and overall groups respectively.

Results: A total of 639 participants (mean age, 46 years \pm 14) with 639 breast lesions (372 benign and 267 malignant lesions) were finally enrolled in this study including 392 participants in the DC and 247 in the VC. In the DC, the optimal viscosity-related parameter in differentiating breast lesions was calculated to be A'-S2-Vmax, with the AUC of 0.88 (95% CI: 0.84, 0.91). Using $>$ 9.97 Pa.s as the cutoff value, the BI-RADS was then modified. The AUC of modified BI-RADS significantly increased from 0.85 (95% CI: 0.81, 0.88) to 0.91 (95% CI: 0.87, 0.93), 0.85 (95% CI: 0.80, 0.89) to 0.90 (95% CI: 0.85, 0.93) and 0.85 (95% CI: 0.82, 0.87) to 0.90 (95% CI: 0.88, 0.92) in the DC, VC and total cohorts respectively ($P < .05$ for all).

Conclusion: The quantitative viscous parameters evaluated by US viscosity imaging contribute to breast cancer diagnosis when combined with BI-RADS.

Key Words: Breast neoplasms; Ultrasonography; Viscosity; Elasticity.

© 2024 The Association of University Radiologists. Published by Elsevier Inc. All rights reserved.

INTRODUCTION

Elasticity assessment of breast lesions has been recommended as an add-on to improve the diagnostic performances of the Breast Imaging Reporting and

Data System (BI-RADS) (1,2). Among various elasticity imaging techniques, shear wave elastography has showed great potentials in breast lesion differentiation by evaluating the propagation of shear waves in soft tissues to acquire the value of Young elastic modulus (3–6). The application of

Acad Radiol xxxx; xx:xxx-xxx

From the Department of Ultrasound, Ruijin Hospital, Shanghai Jiao Tong University School of Medicine, No.197 Ruijin 2nd Road, 200025 Shanghai, China (W.J., S.X., X.J., C.Y., E.C., Y.D., J.Z., Y.J., J.L., Z.T., T.L., X.Z., W.Z., Y.Z., J.Z.); College of Health Science and Technology, Shanghai Jiao Tong University School of Medicine, Shanghai 200025, China (W.J., S.X., Y.D., W.Z., Y.Z., J.Z.); Department of Ultrasound, Nanchang People's Hospital, Nanchang, Jiangxi Province 330000, China (B.T., S.C., M.N.); Department of Ultrasound, Gansu Provincial Cancer Hospital, Lanzhou, Gansu Province, China (L.G., Y.D., M.Z.); Department of Ultrasound, Affiliated Hospital of Guizhou Medical University, Guiyang, Guizhou Province, China (X.C.); Department of Ultrasound, The First Hospital of Jiaxing, Affiliated Hospital of Jiaxing University, Jiaxing, Zhejiang Province, China (H.Z.); Department of Ultrasound, Affiliated Hospital of Yan'an University, Yan'an, Shaanxi Province, China (B.B., H.J.); Department of Ultrasound, Yunnan Kungang Hospital, The Seventh Affiliated Hospital of Daii University, No.2 Ganghenan Road, Anning, Yunnan Province 650330, China (N.L.). Received November 27, 2023; revised February 16, 2024; accepted March 17, 2024. **Address correspondence to:** J.Z. e-mail: zhousu30@126.com

¹ These authors contributed equally.

© 2024 The Association of University Radiologists. Published by Elsevier Inc. All rights reserved.

<https://doi.org/10.1016/j.acra.2024.03.017>

shear wave elastography based on the assumption that the tissues are linearly elastic and homogeneous, which is not in line with the practical situation, because the biological tissues also exhibit viscous behaviors, meaning that waves at different frequencies spread at different phase velocities (7). Thus, the biased estimation is inevitable using the current elastic techniques, especially in the liver and breast (7,8). The viscous properties of tissues can be non-invasively assessed by magnetic resonance elastography in vivo using MRI technique (9), which has been clinically applied not only to stage hepatic fibrosis for patients with chronic liver diseases (10,11) but to characterize benign and malignant breast lesions (12).

Compared to MRI, US is more convenient, less expensive with no contraindications. In addition to the elasticity evaluation, it has emerged as a new tool to quantitatively estimate the viscosity of biological tissues using different parameters (8,13). As shear wave speed varied with frequencies, a fitting dispersion curve can be algorithmically reconstructed using the value of frequencies and varying shear wave velocities, then the slope of this curve, named the shear wave dispersion slope, could be obtained as a viscosity-related parameter (14). Despite the results in patients with primarily viral hepatitis (14), shear-wave dispersion slope has been reported to noninvasively identify lobular inflammation, steatosis and fibrosis for participants with non-alcoholic fatty liver diseases, whether used alone or in conjunction with other indicators (15–17). After liver transplant, the shear-wave dispersion slope was found to be associated with both liver fibrosis and degree of necroinflammation, and thus to detect allograft damage with better diagnostic performance than the liver stiffness value (18). Besides, the viscoelastic response ultrasound, was also proved to be feasible in evaluation of renal transplant status (19).

Despite the extensive research on shear wave elastography (4,20,21), the clinical value of US viscosity imaging has not been well established previously in breast lesion differentiation in vivo. There were different rheological models to parametrize the frequency-dependent phase velocity (8), and the Voigt model seemed to be more appropriate for the description of viscous effects (22). Until now, only one very small sample study has preliminarily identified the potential value of Voigt model-based shear viscosity in the diagnosis of breast malignancies, in which the Voigt model-based shear viscosity was 8.22 ± 3.36 Pa.s for the malignant breast tumors and 2.83 ± 1.47 Pa.s for the benign ones, showing a significant difference (8). Therefore, large-sample, multi-center studies are warranted not only to choose the most optimal quantitative viscous parameter in differentiation of breast masses, but also to explore the clinical value of viscous properties assessed by US viscosity imaging.

In this study, all participants were divided into the development cohort (DC) and the validation cohort (VC) according to their participating time. At first, the state-of-art US viscosity imaging technology was used in the DC to obtain the quantitative viscous parameters of breast lesions, including both the shear wave dispersion and Voigt model-based viscosity coefficients. Then the diagnostic performances of all viscosity parameters were calculated to select the optimal one in differentiating

breast lesions with different sizes. Subsequently, the cutoff value of the optimal viscosity parameter was calculated and used to modify the original BI-RADS to explore whether this combination would improve the diagnostic efficiency of the BI-RADS alone. Finally, the acquired optimal viscous parameter in the DC was used for validation of the results in the VC and the total cohorts. In brief, the diagnostic value of the viscous properties in characterization of breast lesions was explored and then demonstrated in this multi-center study.

MATERIALS AND METHODS

Study Design

This prospective study was conducted at six hospitals (Ruijin Hospital, Shanghai Jiao Tong University School of Medicine; The Affiliated Hospital of Guizhou Medical University; Gansu Provincial Cancer Hospital; The Third hospital of Nanchang; The First Hospital of Jiaxing; Yanan University Affiliated Hospital) in China. The research conformed to the ethical standards approved by the Ethic Committee and all participants signed the informed consent. From June 2021 to November 2022, 687 participants who were hospitalized in the participating centers underwent preoperative US, US viscosity imaging examination, and the subsequent core needle biopsy or surgery for their breast lesions. The inclusion criteria were (a) age ≥ 18 years old; (b) male or female; (c) not in pregnancy or lactation; (d) no implantation of breast prostheses; (e) with ultrasound detectable solid or solid-predominant breast lesions; (f) with qualified viscous images. The exclusion criteria were (a) unsatisfactory US images; (b) with history of breast surgery on the affected side, neoadjuvant chemotherapy or systemic chemoradiotherapy; (c) breast lesions with numerous coarse calcifications; (d) no definite histological diagnosis. One lesion per patient was included. For patient with multiple lesions, the one with the highest BI-RADS classification was selected, and for the lesions with the same BI-RADS classification, the one with the best viscous images of quality control would be selected.

Totally, 687 participants meeting the inclusion criteria were recruited in this study, and 48 were excluded for unsatisfactory images ($n = 30$), having received treatment before ($n = 8$), breast lesions with numerous coarse calcifications ($n = 5$) and no final diagnosis ($n = 5$). Therefore, 639 eligible participants were finally enrolled. They were divided into two cohorts, with 392 participants enrolled between June 2021 and February 2022 serving as the DC, and 247 participants enrolled between March 2022 and August 2022 serving as the VC (Fig 1).

Imaging Protocol and Data Analysis

The research protocol for the DC was the same as the VC. In the beginning, radiologists of all participating hospitals have received strict training for standardized operational procedures. Conventional breast US was first performed (23) based on the American Institute of Ultrasound in Medicine

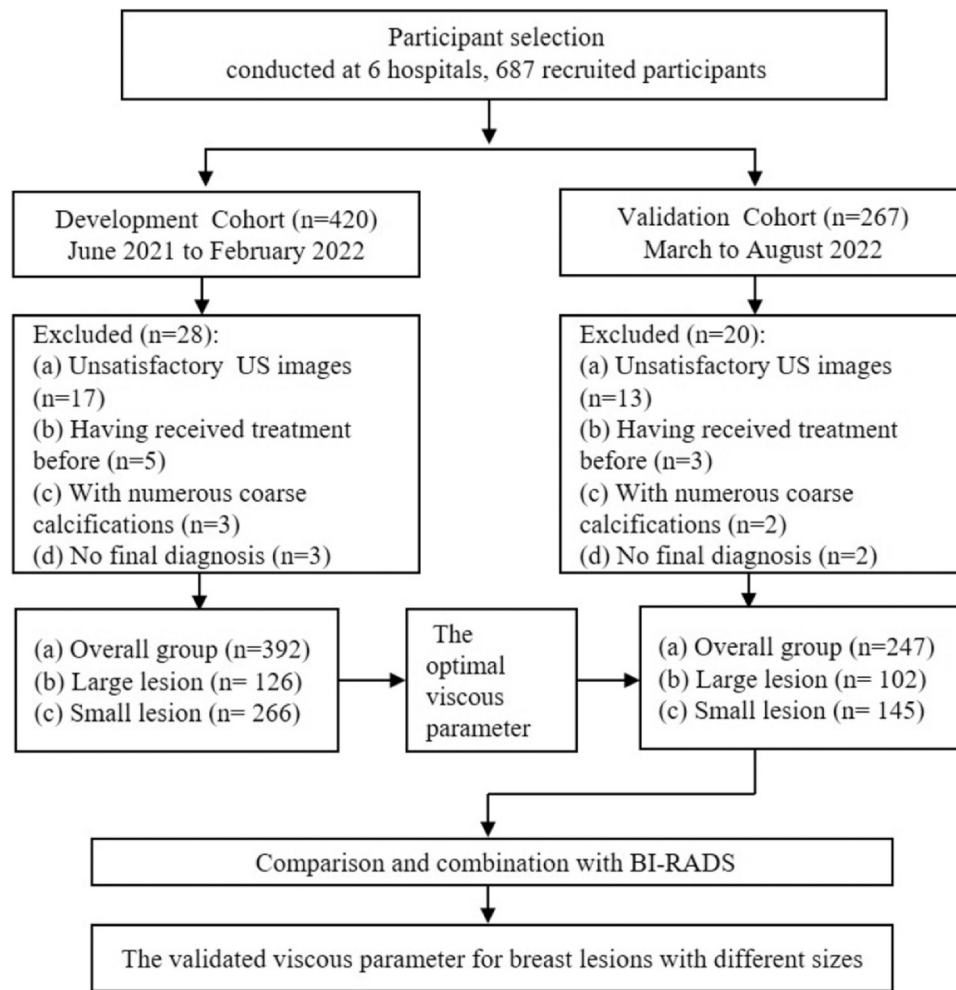


Figure 1. The flowchart of study procedure.

practice guidelines using the linear array probe (3–11 MHz or 4–15 MHz) of the Resona 9 (Mindray, Shenzhen, China) ultrasound system to determine the target lesion, which was given a BI-RADS category (including categories 3, 4A, 4B, 4C and 5) by the radiologist who performed the examination. There were 12 radiologists participating in the operation of US examination, and each one with more than 5 years of experience in breast US. The radiologists were independent of any clinical or other imaging findings. Then the US viscosity imaging examination with the probe (3–11 MHz) was initiated, during which the participants were asked to hold their breath and the probe was stabilized with as little pressure as possible to obtain the satisfactory images that met the quality control requirements (Fig 2). The first 30 operations of each radiologist were not included in this study.

When satisfied images were acquired, a square region of interest (ROI) was set for the viscous acquisition, it should be standardized with the scope from the subcutaneous fat layer to the pectoral muscle layer, and the lateral margin should encompass at least 3 mm of the surrounding tissue around the breast lesions by adjusting the position and

scanning angle of the probe. The US viscosity imaging function was then activated, and the gray-scale US image and the color-coded US viscosity images were displayed simultaneously on the screen. By manually drawing the lesion contour in the gray-scale US image, the Voigt model-based parameters including the maximum value (V_{max}), mean value (V_{mean}), minimum value (V_{min}) and standard deviation (V_{sd}) and the shear wave dispersion coefficients including the maximum value (D_{max}), mean value (D_{mean}), minimum value (D_{min}) and standard deviation (D_{sd}) were automatically acquired using the built-in software of Resona 9 ultrasound system. The corresponding viscosity parameters were also automatically obtained for the peritumoral region, using the system's measurement tool known as “Shell” (24), the thickness of which can be manually adjusted.

To be specific, the Voigt model-based parameters V_{max} , V_{mean} , V_{min} and V_{sd} were obtained for the tumor itself (Fig 3a). The S_n - V_{max} , S_n - V_{mean} , S_n - V_{min} , S_n - V_{sd} and A' - S_n - V_{max} , A' - S_n - V_{mean} , A' - S_n - V_{min} , A' - S_n - V_{sd} were acquired for the peritumoral region, among which n represented the thickness of shell, and it was fixed as 1 mm or 2 mm in this study. Besides, S_n stood for parameters obtained

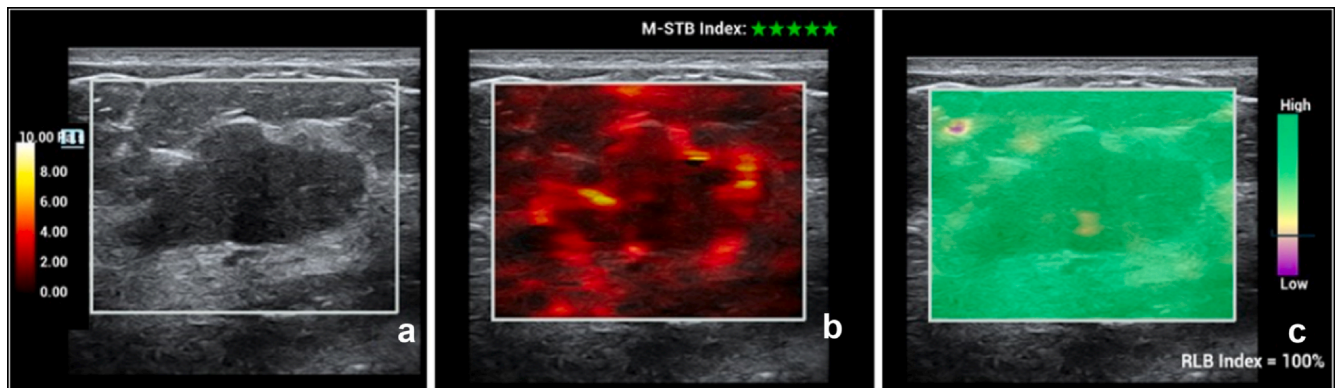


Figure 2. The quality control of viscous images. (a) The grayscale US images of a hypochoic breast lesion. (b) The M-STB index of the images, five consecutive green stars meaning the images were collected in a stable state. (c) The RLB Map and the RLB index of the images. Areas with high reliability were shown in green, and areas with low reliability were shown in purple. RLB index showed the reliability degree of the current image in percentage, and white indicated qualified reliability. M-STB index, motion stability index; RLB Map, reliability map; RLB index, reliability index. (Color version of figure is available online.)

only within the region of the corresponding shell, while $A'-S_n$ meant the value encompassing both the lesion and corresponding shell (Fig 3c and e). Similarly, the naming of parameters for the shear wave dispersion coefficients also followed this principle (Fig 3b, d and f). Finally, all US images and viscous parameters were digitally stored on the hard disk of the US system, and then exported for further offline analysis.

Exploration of the Optimal Viscous Parameters in the DC

The diagnostic performances of all viscous parameters were calculated using the receiver operating curve (ROC) in the DC. By comparing the areas under the ROC curves (AUC) of various viscous parameters, the one with the highest AUC was considered as the optimal viscous parameter and used for further breast lesion discrimination. Then the cutoff value of this parameter in differentiation of breast lesion was statistically calculated for further modification of BI-RADS. In detail, if the optimal parameter of the breast lesion was larger than the cutoff value, the BI-RADS category would upgrade, and if it was less than the cutoff value, the BI-RADS remain unchanged. Additionally, BI-RADS category 5 would not upgrade whether the parameter was (4). Then the original and modified BI-RADS was statistically compared.

In the DC, VC and total cohorts, all breast lesions were divided into three groups based on the mean diameters of them: the overall group (no matter what the maximum diameter was), the large lesion group (the maximum diameter > 20 mm) and the small lesion group (the maximum diameter ≤ 20 mm), besides, 20 mm was used for grouping because T1 or T2 staging of breast cancer was also based on it by AJCC (25). The diagnostic performances of the optimal viscous parameter, BI-RADS and modified BI-RADS were evaluated in these three groups in the DC, VC and total cohorts.

Validation of the Optimal Viscous Parameters in the VC and Total Cohorts

In the VC, there were also the overall, large lesion and small lesion groups using the same criteria as DC. The diagnostic performances of the optimal parameter in DC were validated in different groups of the VC and total cohorts, and were also compared and combined with BI-RADS.

The Reproducibility of US Viscosity Imaging

In a separate cohort of 50 breast lesions in 50 patients, the reproducibility was evaluated by two radiologists (W.R.J and X.H.J, each one with more than 10 years of experience in breast US). Followed by the previously mentioned procedure, the two radiologists independently performed the US viscosity imaging to obtain all viscous parameters for the same breast mass. All parameters were then stored for further calculation of interobserver variability.

The Reference Standard

All participants underwent surgery or core needle biopsy for the target lesion after US imaging. The histologic results of breast lesions would be used as the reference standard. The breast pathologists with more than 15 years of experience made the final diagnosis without any information of US or other images.

Statistical Analysis

The SPSS version 21.0 (SPSS Inc., Chicago, IL, USA) and MedCalc 19.05 (Med-Calc Software, Mariakerke, Belgium) were used for statistical analysis. The Mann-Whitney U-test, independent t-test and Chi-square test were used for statistical comparison. A level of $P < .05$ was considered statistically significant. With histological results as reference standard, ROC curve was used to calculate the AUC,

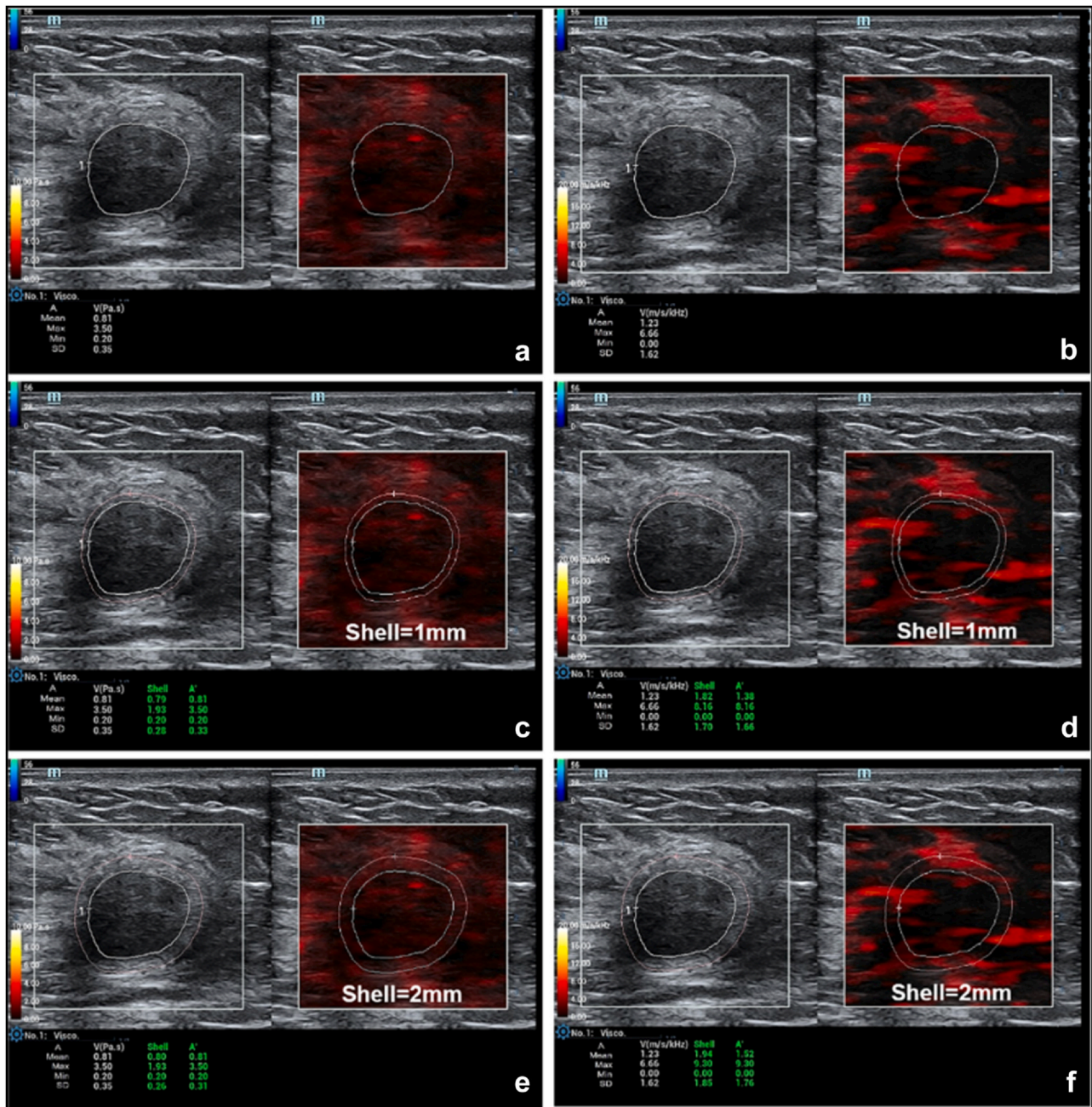


Figure 3. The example of all viscous parameters of one breast lesion using US viscosity imaging. **(a)** The Voigt model-based parameters (Pa.s) and **(b)** shear wave dispersion coefficients (m/s/kHz) of breast lesion itself (Vmean, Vmax, Vmin, Vsd and Dmean, Dmax, Dmin, Dsd). **(c)** The Voigt model-based parameters and **(d)** shear wave dispersion coefficients of breast lesions with shell = 1 mm (S1-Vmean, S1-Vmax, S1-Vmin, S1-Vsd and A'-S1-Vmean, A'-S1-Vmax, A'-S1-Vmin, A'-S1-Vsd and S1-Dmean, S1-Dmax, S1-Dmin, S1-Dsd and A'-S1-Dmean, A'-S1-Dmax, A'-S1-Dmin, A'-S1-Dsd). **(e)** The Voigt model-based parameters and **(f)** shear wave dispersion coefficients of breast lesions with shell = 2 mm (S2-Vmean, S2-Vmax, S2-Vmin, S2-Vsd and A'-S2-Vmean, A'-S2-Vmax, A'-S2-Vmin, A'-S2-Vsd and S2-Dmean, S2-Dmax, S2-Dmin, S2-Dsd and A'-S2-Dmean, A'-S2-Dmax, A'-S2-Dmin, A'-S2-Dsd). Dmax, maximum value of shear wave dispersion coefficients; Dmean, mean value of shear wave dispersion coefficients; Dmin, minimum value of shear wave dispersion coefficients; Dsd, standard deviation of shear wave dispersion coefficients; Vmax, maximum value of Voigt model-based parameters; Vmean, mean value of Voigt model-based parameters; Vmin, minimum value of Voigt model-based parameters; Vsd, standard deviation of Voigt model-based parameters.

sensitivity and specificity of all parameters. The cutoff values were determined using the Youden index, and the AUCs of different variables were compared using the method

proposed by DeLong et al (26). Intra-class correlation coefficient (ICC) was used for evaluation of the reproducibility between two radiologists.

RESULTS

Participant Characteristics

Of 639 participants (mean age, 46 years \pm 14; 638 women) with breast lesions, 372 (58.2%) were benign and 267 (41.8%) were malignant. The mean value of maximum diameter was 20.5 mm \pm 10.7 (range, 4.4–113.7 mm). In terms of age ($P = .68$, $P = .20$ and $P = .51$), the maximum diameter ($P = .51$, $P = .77$ and $P = .28$), and pathological diagnosis ($P = .65$, $P = .41$ and $P = .97$), we found no evidence of a difference between the DC and VC (Table 1). The distribution of BI-RADS is displayed in Table S1.

Histological Diagnosis

Histological results were acquired for all breast lesions. Of all malignant ones, the proportion of invasive ductal carcinoma, ductal carcinoma in situ and solid papillary carcinoma were 80.1% (129/161), 10.6% (17/161), 3.7% (6/161) and 77.4% (82/106), 13.2% (14/106), 5.7% (6/106) in the DC and VC respectively, while of all benign ones, fibroadenoma, adenosis and intraductal papilloma accounted for 54.5% (126/231), 26.4% (61/231), 11.3% (26/231) and 58.9% (83/141), 22.7% (32/141), 12.8% (18/141) in the DC and VC respectively (Table S2).

Exploration of the Optimal Viscous Parameters in the DC

The diagnostic performances of all viscous parameters in differentiation of breast lesions are displayed in Table 2. Of all Voigt model-based parameters (Pa.s), A'-S2-Vmax showed the highest AUC of 0.88 (95% CI: 0.84, 0.91) in differentiating benign and malignant breast lesions, while of all significant shear wave dispersion coefficients (m/s/kHz), Dmax had the highest AUC of 0.83 (95% CI: 0.79, 0.86). Therefore, the A'-S2-Vmax that showed the highest AUC was finally chosen as the optimal viscous parameter for further analysis. Using A'-S2-Vmax > 9.97 Pa.s as the cutoff value, the sensitivity and specificity were 80% (128 of 161), and 79% (182 of 231) respectively for the overall group in the DC (Table 2). Furthermore, the mean value of A'-S2-Vmax was proved to be significantly different between the large and small lesion groups (11.7 Pa.s \pm 5.1 vs. 7.8 Pa.s \pm 4.7, $P < .001$), with the AUC of 0.73 (95% CI: 0.65, 0.79) and 0.79 (95% CI: 0.73, 0.84) respectively.

The Diagnostic Performances of A'-S2-Vmax, BI-RADS and Modified BI-RADS in the DC

The malignancy rate was 41.4% (161 of 392), 59.6% (99 of 166) and 27.4% (62 of 226) in the overall, large lesion and small lesion group of the DC. Using the cutoff value above, the viscous parameter A'-S2-Vmax was combined with BI-RADS for a comparison (Table 3). The AUC of modified BI-RADS improved from 0.85 (95% CI: 0.81, 0.98) to 0.91 (95% CI: 0.87, 0.93) in the overall group, from 0.84 (95% CI: 0.78, 0.90) to 0.89 (95% CI: 0.83, 0.93) in the large

TABLE 1. Participant Characteristics

	Overall Group (n = 639)		Large lesion group (n = 268)		Small lesion group (n = 371)		P value
	DC (n = 392)	VC (n = 247)	DC (n = 166)	VC (n = 102)	DC (n = 226)	VC (n = 145)	
Age (y)*	46 \pm 14 (19–84)	46 \pm 15 (18–89)	47 \pm 15 (19–84)	49 \pm 17 (18–89)	45 \pm 13 (21–83)	44 \pm 14 (19–78)	.51
Diameter (mm)*	20.7 \pm 10.4 (4.4–68)	20.1 \pm 11.3 (5.2–113.7)	30.3 \pm 8.6 (20.1–68)	29.9 \pm 11.3 (20.2–113.7)	13.8 \pm 4.1 (4.4–20)	13.3 \pm 3.8 (5.2–20)	.28
Pathological diagnosis†							.97
Benign	231 (36.2%)	141 (22.1%)	67 (25.0%)	36 (13.4%)	164 (44.3%)	105 (28.3%)	
Malignant	161 (25.2%)	106 (16.6%)	99 (36.9%)	66 (24.6%)	62 (16.7%)	40 (10.8%)	

*data are the mean \pm standard deviation with the range in parentheses.

†data are numbers of participants, and data in parentheses are percentages DC, development cohort; VC, validation cohort.

TABLE 2. The Diagnostic Performances of All Viscous Parameters in the Development Cohort Using US Viscosity Imaging

	P value	Cutoff value	AUC	Sensitivity (%)	Specificity (%)
<i>Visco (Pa.s)</i>					
Vmean	< .001	> 2.24	0.71 [0.66–0.76]	53 (86/161)	79 (182/231)
Vmax	< .001	> 9.73	0.86 [0.82–0.89]	72 (116/161)	84 (194/231)
Vmin	< .001	≤ 0.18	0.67 [0.62–0.72]	65 (104/161)	70 (161/231)
Vsd	< .001	> 1.39	0.83 [0.79–0.87]	69 (111/161)	81 (188/231)
S1-Vmean	< .001	> 2.42	0.82 [0.78–0.86]	73 (118/161)	76 (175/231)
S1-Vmax	< .001	> 6.90	0.86 [0.82–0.89]	89 (143/161)	69 (179/231)
S1-Vmin	.009	≤ 0.09	0.58 [0.53–0.63]	44 (71/161)	77 (179/231)
S1-Vsd	< .001	> 1.52	0.85 [0.81–0.88]	78 (126/161)	76 (176/231)
A'-S1-Vmean	< .001	> 1.91	0.74 [0.70–0.79]	76 (122/161)	64 (147/231)
A'-S1-Vmax	< .001	> 9.73	0.87 [0.83–0.90]	76 (122/161)	81 (186/231)
A'-S1-Vmin	< .001	≤ 0	0.66 [0.61–0.71]	60 (97/161)	72 (167/231)
A'-S1-Vsd	< .001	> 1.44	0.84 [0.80–0.88]	74 (119/161)	79 (183/231)
S2-Vmean	< .001	> 1.86	0.83 [0.79–0.87]	88 (142/161)	61 (140/231)
S2-Vmax	< .001	> 6.81	0.86 [0.83–0.90]	93 (149/161)	65 (150/231)
S2-Vmin	< .001	≤ 0	0.61 [0.56–0.66]	54 (87/161)	72 (166/231)
S2-Vsd	< .001	> 1.44	0.85 [0.82–0.89]	80 (128/161)	76 (176/231)
A'-S2-Vmean	< .001	> 1.94	0.77 [0.73–0.81]	76 (122/161)	66 (152/231)
A'-S2-Vmax	< .001	> 9.97	0.88 [0.84–0.91]	80 (128/161)	79 (182/231)
A'-S2-Vmin	< .001	≤ 0	0.66 [0.61–0.71]	70 (112/161)	64 (147/231)
A'-S2-Vsd	< .001	> 1.17	0.85 [0.81–0.89]	88 (141/161)	66 (153/231)
<i>Disper (m/s/kHz)</i>					
Dmean	.89				
Dmax	< .001	> 14.01	0.83 [0.79–0.86]	78 (125/161)	77 (177/231)
Dmin	.11				
Dsd	< .001	> 2.24	0.76 [0.71–0.80]	83 (133/161)	59 (136/231)
S1-Dmean	< .001	> 3.16	0.68 [0.63–0.72]	72 (116/161)	56 (130/231)
S1-Dmax	< .001	> 13.15	0.85 [0.81–0.88]	83 (133/161)	75 (173/231)
S1-Dmin	.02	≤ 0.02	0.53 [0.47–0.58]	98 (158/161)	7 (17/231)
S1-Dsd	< .001	> 2.73	0.84 [0.80–0.87]	87 (140/161)	71 (165/231)
A'-S1-Dmean	.27				
A'-S1-Dmax	< .001	> 13.01	0.84 [0.80–0.87]	87 (140/161)	67 (154/231)
A'-S1-Dmin	.21				
A'-S1-Dsd	< .001	> 2.85	0.79 [0.75–0.83]	75 (120/161)	75 (173/231)
S2-Dmean	< .001	> 3.43	0.69 [0.64–0.73]	65 (104/161)	67 (155/231)
S2-Dmax	< .001	> 16.21	0.85 [0.81–0.88]	75 (120/161)	83 (191/231)
S2-Dmin	.004	≤ 0	0.52 [0.47–0.57]	100 (161/161)	3 (8/231)
S2-Dsd	< .001	> 2.76	0.84 [0.80–0.88]	87 (140/161)	71 (164/231)
A'-S2-Dmean	.02	> 4.26	0.57 [0.52–0.62]	31 (50/161)	85 (196/231)
A'-S2-Dmax	< .001	> 16.55	0.84 [0.80–0.88]	77 (124/161)	79 (182/231)
A'-S2-Dmin	.013	≤ 0	0.51 [0.46–0.56]	100 (161/161)	2 (4/231)
A'-S2-Dsd	< .001	> 2.55	0.81 [0.77–0.85]	86 (139/161)	63 (146/231)

Data in parentheses are numerators/denominators; data in brackets are 95% CIs.

AUC, area under the receiver operating characteristic curve.

lesion group and from 0.82 (95% CI: 0.76, 0.86) to 0.90 (95% CI: 0.85, 0.93) in the small lesion group, with significant difference for all groups ($P < .001$, = .006 and $< .001$, respectively) (Fig. 4–6).

The Diagnostic Performances in the VC

The malignancy rate was 42.9% (106 of 247), 64.7% (66 of 102) and 27.6% (40 of 145) in the overall, large lesion and small lesion group of the VC. The mean value of Voigt

model-based parameter A'-S2-Vmax was also significantly different between benign and malignant breast lesions in all three groups of the VC ($P < .001$ for all comparisons) with the AUC of 0.78 (95% CI: 0.74, 0.81), 0.71 (95% CI: 0.65, 0.76) and 0.77 (95% CI: 0.73, 0.82). When further combined with BI-RADS, the AUC were significantly increased from 0.85 (95% CI: 0.80, 0.89) to 0.90 (95% CI: 0.85, 0.93) for the overall group ($P = .002$), and from 0.81 (95% CI: 0.74, 0.87) to 0.87 (95% CI: 0.80, 0.92) for the small lesion group ($P = .02$) (Table 4, Fig 6).

TABLE 3. The Diagnostic Performances of BI-RADS and Modified BI-RADS in the Development Cohort

	<i>P</i> value*	AUC	Sensitivity (%)	Specificity (%)	<i>P</i> value vs. BI-RADS†
Overall Group					
BI-RADS	< .001	0.85 [0.81–0.88]	92 (148/161)	61 (141/231)	
Modified BI-RADS	< .001	0.91 [0.87–0.93]	84 (135/161)	81 (187/231)	< .001
Large lesion group					
BI-RADS	< .001	0.84 [0.78–0.90]	96 (95/99)	57 (38/67)	
Modified BI-RADS	< .001	0.89 [0.83–0.93]	89 (88/99)	69 (46/67)	.006
Small lesion group					
BI-RADS	< .001	0.82 [0.76–0.86]	85 (53/62)	63 (103/164)	
Modified BI-RADS	< .001	0.90 [0.85–0.93]	76 (47/62)	86 (141/164)	< .001

Data in parentheses are numerators/denominators; data in brackets are 95% CIs.

AUC, area under the receiver operating characteristic curve; BI-RADS, breast imaging reporting and data system.

* Statistical difference between benign and malignant breast lesions.

† Statistical difference between BI-RADS and modified BI-RADS.

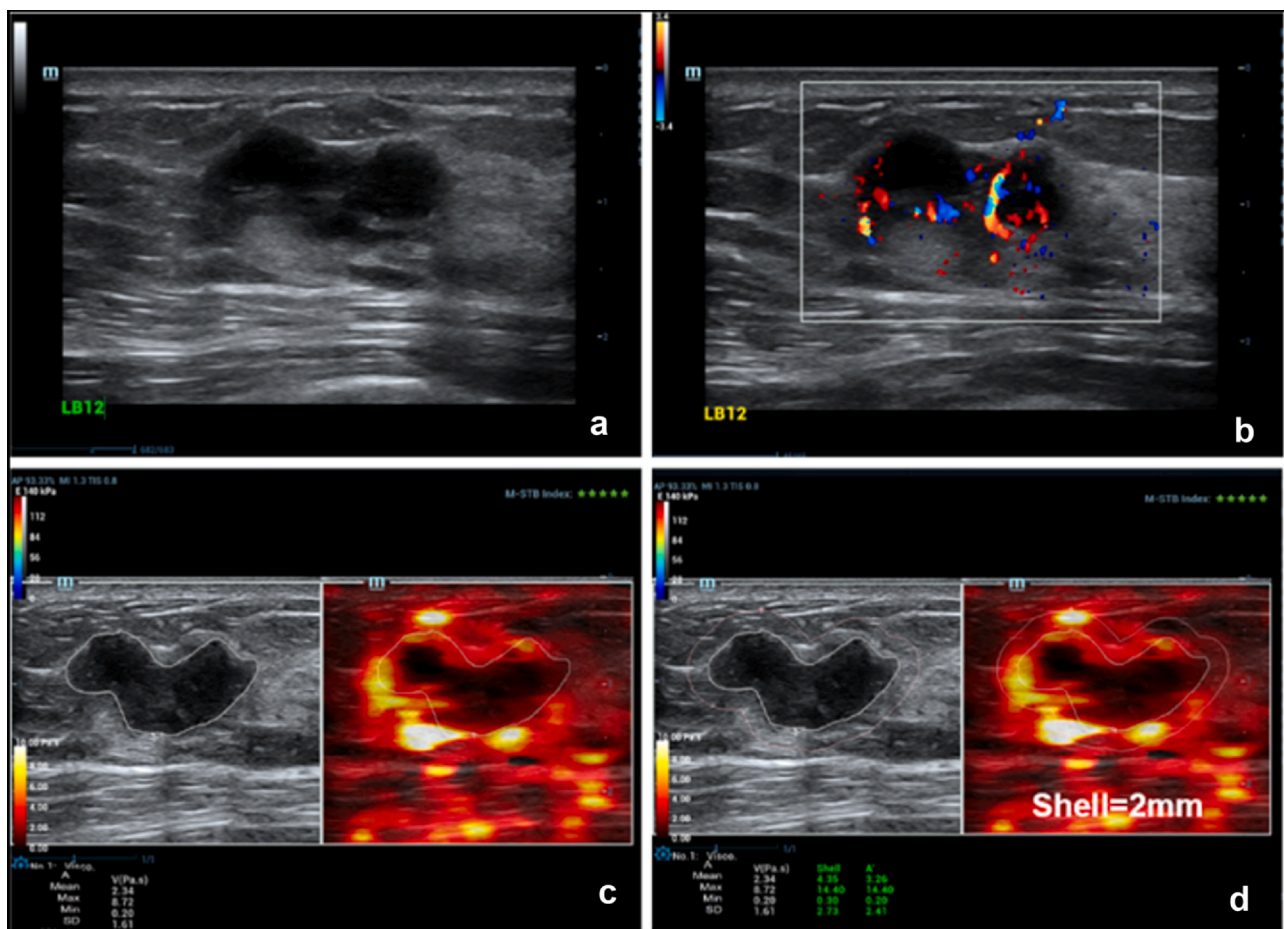


Figure 4. Invasive ductal carcinoma of a 52-year-old female in the left breast. Conventional US showed a hypoechoic lesion with irregular shape, indistinct margin (a) internal and peripheral vascularity (b), and the final diagnosis was BI-RADS 4B. US viscosity imaging showed the viscous parameters of the lesion itself (c) and the value of A'-S2-Vmax was 14.40 Pa.s, which was larger than the cutoff value of 9.97 Pa.s, so the modified BI-RADS improved from 4B to 4C.

The Diagnostic Performances in the Total Cohorts

In the total cohorts of 639 breast lesions, the AUC was 0.78 (95% CI: 0.74, 0.81) for the overall group using A'-S2-

Vmax > 9.97 Pa.s as the cutoff value. When combined with BI-RADS, the AUC significantly increased from 0.85 (95% CI: 0.82, 0.87) to 0.90 (95% CI: 0.88, 0.92), 0.85 (95% CI: 0.80, 0.92) to 0.89 (95% CI: 0.84, 0.92) and 0.81 (95%

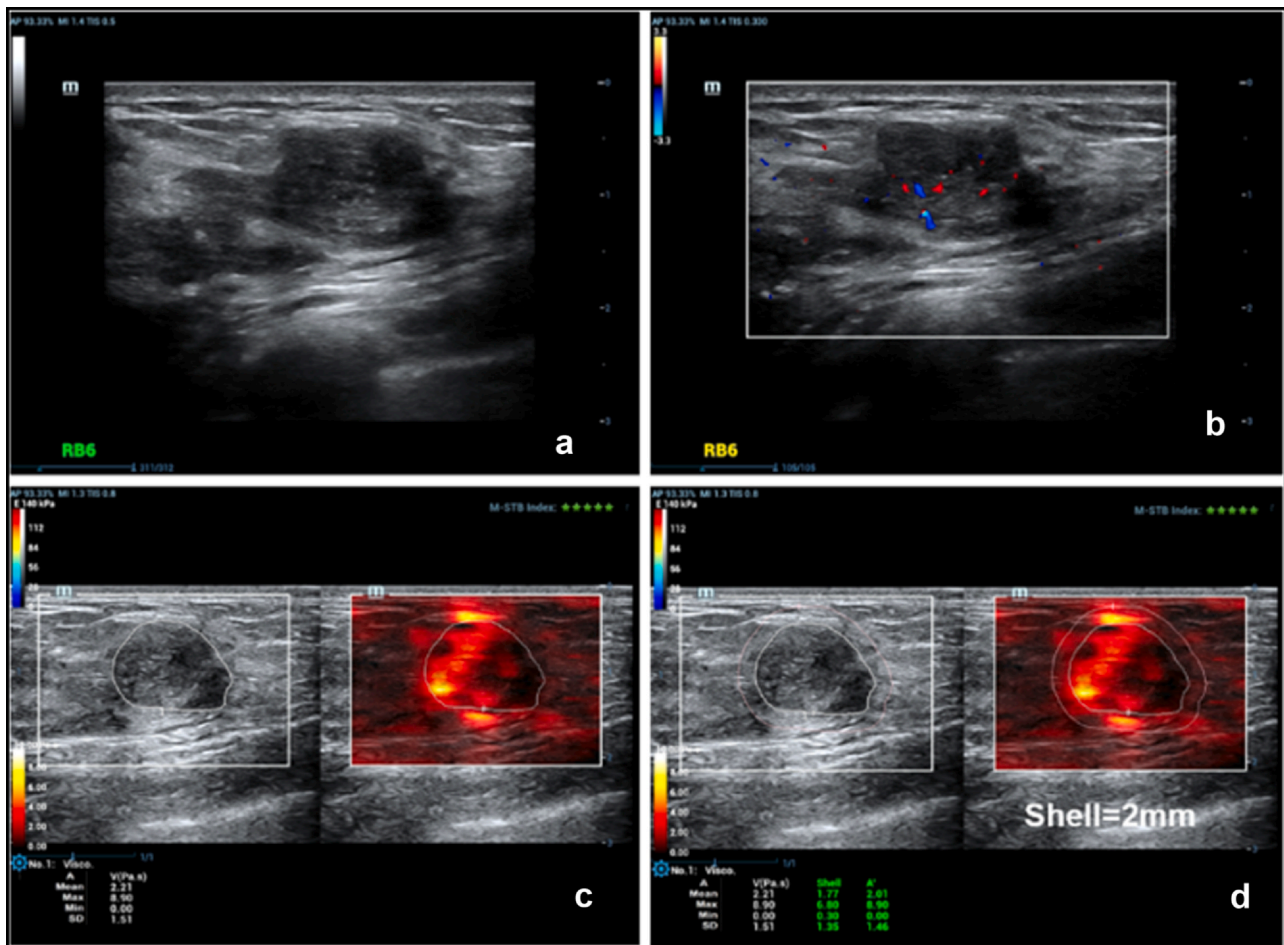


Figure 5. Fibroadenoma of a 26-year-old female in the right breast. Conventional US showed a hypoechoic lesion with irregular shape, angular margin (a) and internal vascularity (b), and the final diagnosis was BI-RADS 4A. US viscosity imaging showed the viscous parameters of the lesion itself (c), and the value of $A'-S2-V_{max}$ was 8.90 Pa.s, which was less than the cutoff value of 9.97 Pa.s, so BI-RADS did not downgrade.

CI: 0.77, 0.85) to 0.88 (95% CI: 0.85, 0.92) for the overall ($P < .001$), large lesion ($P = .006$) and small lesion groups ($P < .001$) respectively (Table S3).

The Reproducibility of US Viscosity Imaging

As for the optimal Voigt model-based parameter $A'-S2-V_{max}$, there was an excellent reproducibility between the two radiologists with the ICC value of 0.855.

DISCUSSION

Biological tissues are not just linearly elastic or homogeneous medium, but more complicated with viscous properties (7), meaning that the shear wave speed varies with different frequencies during propagation. Theoretically, quantitative viscosity-based parameters may better reflect the real characteristics of breast lesions. However, the related clinical research of US viscosity imaging is rare and no multicenter studies have been conducted until now (8,27). Our study found that of all viscous parameters, Voigt model-based A' -

$S2-V_{max}$ showed the highest AUC of 0.88 ($P < .001$). Furthermore, when this selected parameter was combined with BI-RADS, the AUCs of modified BI-RADS were significantly increased from 0.85 to 0.91 in the DC ($P < .001$), from 0.85 to 0.90 in the VC ($P = .002$), and from 0.85 to 0.90 in the total cohorts ($P < .001$).

There were different models for evaluating viscous property of biological tissues using US viscosity imaging. Kumar et al. has explored the value of Voigt model-based shear viscosity in 43 female patients with suspicious breast masses by US and found a significant difference between malignant and benign lesions (8). In our study, the diagnostic performance of V_{max} was significantly better than D_{max} of shear wave dispersion ($P = .02$), and $A'-S2-V_{max}$ had the highest AUC among all viscosity parameters. Shear wave dispersion is more commonly used in the liver using the phase-difference method to estimate the dispersion slope of shear wave speed at different frequencies (28), while the Voigt model using a more complex equation to illustrate the frequency-dependent speed, including the factors of density, elasticity and viscosity of the medium (28), which may

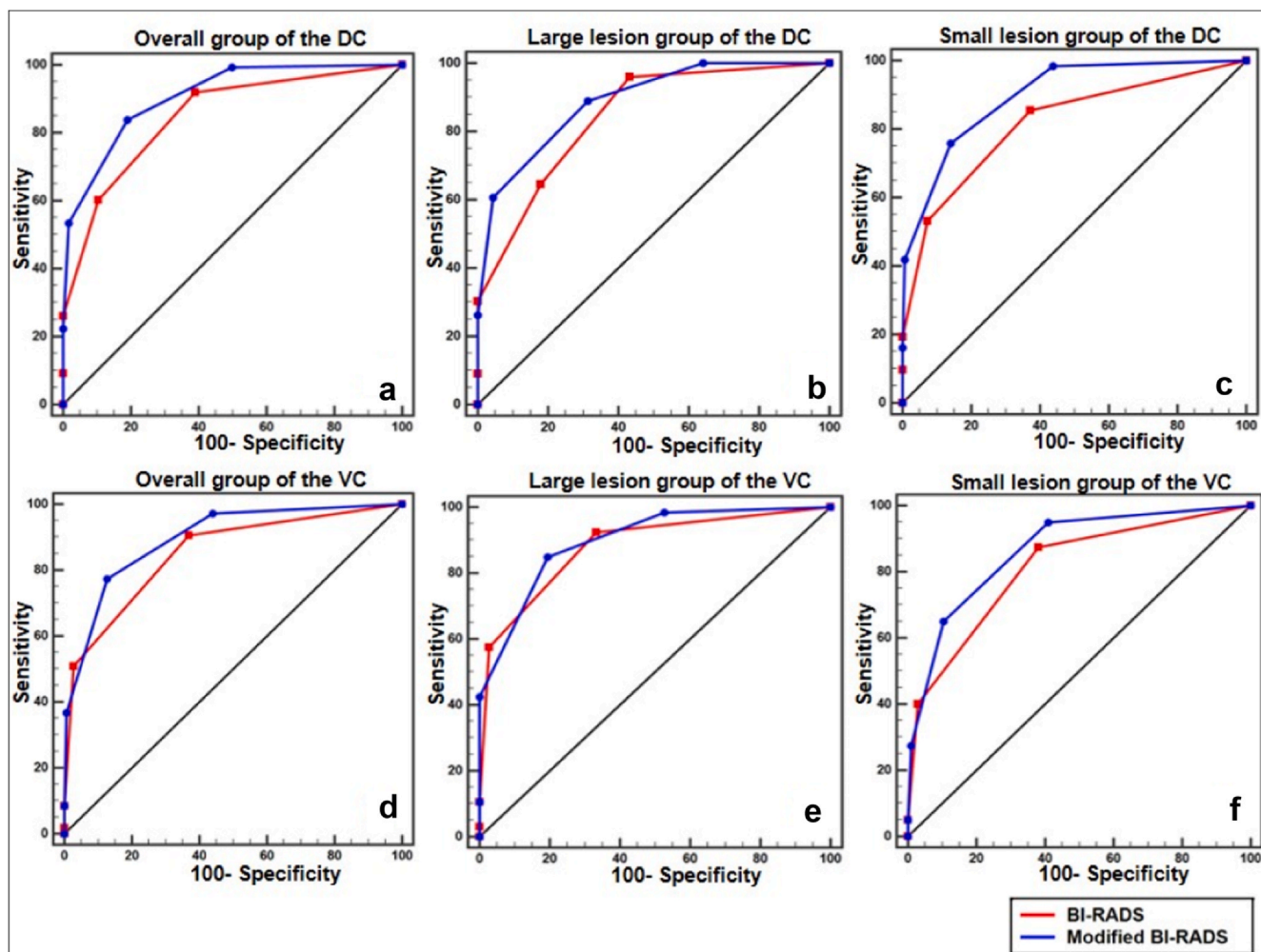


Figure 6. The ROCs of BI-RADS and modified BI-RADS in all groups of the DC and VC. (a–c) The ROC of BI-RADS and modified BI-RADS in overall (a), large lesion (b) and small lesion (c) groups of the DC ($P < .001$, = .006, < .001 respectively). (d–f) The ROC of BI-RADS and modified BI-RADS in overall (d), large lesion (e) and small lesion (f) groups of the VC ($P = .002$, = .39, < .02 respectively). DC, development cohort; ROC, receiver operating curve, VC, validation cohort.

TABLE 4. The Diagnostic Performances of BI-RADS and Modified BI-RADS in the Validation Cohort

	<i>P</i> value*	AUC	Sensitivity (%)	Specificity (%)	<i>P</i> value vs. BI-RADS†
Overall Group of the VC					
BI-RADS	< .001	0.85 [0.80–0.89]	91 (96/106)	63 (89/141)	
Modified BI-RADS	< .001	0.90 [0.85–0.93]	77 (82/106)	87 (123/141)	.002
Large lesion group of the VC					
BI-RADS	< .001	0.88 [0.80–0.94]	92 (61/66)	67 (24/36)	
Modified BI-RADS	< .001	0.90 [0.82–0.95]	85 (56/66)	81 (29/36)	.39
Small lesion group of the VC					
BI-RADS	< .001	0.81 [0.74–0.87]	88 (35/40)	62 (65/105)	.02
Modified BI-RADS	< .001	0.87 [0.80–0.92]	65 (26/40)	90 (94/105)	

Data in parentheses are numerators/denominators; data in brackets are 95% CIs.

AUC, area under the receiver operating characteristic curve; BI-RADS, breast imaging reporting and data system.

* Statistical difference between benign and malignant breast lesions.

† Statistical difference between BI-RADS and modified BI-RADS.

explain the superior diagnostic performance of the Voigt model-based parameter in breast lesions compared to the shear wave dispersion. The mean value of malignant masses ($13.88 \text{ Pa}\cdot\text{s} \pm 4.64$) was higher than that of benign ones ($6.84 \text{ Pa}\cdot\text{s} \pm 3.88$) in our study, which was consistent with the former results, suggesting that malignant breast lesions were more viscous than benign ones (8,29–31). On one hand, the increased viscosity of breast cancer may result from desmoplasia reaction, which increased the density of collagen and fibronectin, and reduced the density of associated proteoglycan molecule (32); on the other hand, it may also correlate with the heterogeneity of malignant tissues (29,33).

An interesting finding of this study was that the diagnostic performances of peritumor viscosity parameters were better than those of tumor itself, which had never been reported. Our results showed that the $A'-S2-V_{\text{max}}$ (representing the viscosity parameter of the 2 mm peritumor tissue) had the best diagnostic performance, which may be related to the “stiff rim sign” in breast shear wave elastography. The stiff rim sign of malignant breast tumor has been proposed by Zhou et al using shear wave elastography (4), and malignant tumors with the stiff rim were demonstrated to be larger and more aggressive (34). The possible reason may be the infiltration of malignant growth or desmoplasia of the surrounding stroma, which altered the structure of collagenous extracellular matrix, and thus modified the viscoelastic properties (32,34). As tumor size played a role in determining the stiffness of a tumor, we also found a significant difference in the viscous parameters between the large lesion ($> 20 \text{ mm}$) and small lesion groups ($\leq 20 \text{ mm}$), implying that the viscous features of tumor evaluated by US viscosity imaging also related with the intrinsic tumor biologic factors (35).

In this research, the AUC was higher in the large lesion group than in the small lesion group both in DC (0.84 vs. 0.82) and VC (0.88 vs. 0.81), meaning that the diagnostic efficiency of BI-RADS was better for large masses. When combined with viscous parameter, the AUCs of modified BI-RADS were improved for all three groups, and it seemed to be more obvious in the small lesion group. Tumor diameter was an important factor for tumor staging, treatment and prognosis (25), therefore, the viscous properties may provide more clinical information for an individualized strategy of the patients, and further researches were required to investigate the association between the viscosity imaging and other biological characteristics. US played a crucial role in breast lesion differentiation with higher sensitivity but lower specificity (36). The malignancy rate decreased from 9.0% (23/253) to 2.0% (4/199) for primary and modified BI-RADS 3 lesions, and from 44.9% (93/207) to 28.6% (46/161) for primary and modified BI-RADS 4A lesions (Table S1), which was closer to the rate of American College of Radiology (2). To be mentioned, the specificity of modified BI-RADS increased from 62% (230/372) to 83% (310/372), meaning that 80 participants may avoid surgical procedures, including 13 large and 67 small lesions (Table S3).

There were some limitations in this study. First, all participants were those who intended to undergo a surgery or core needle biopsy, so the selective bias was inevitable. Second, of all Voigt-model and shear wave dispersion parameters, the one with the highest AUC was chosen for the following research, the value of other parameters may also need further studies. Third, many factors may affect the propagation of shear waves, such as the thickness and status of gland, the depth and location of breast lesions, which should also be incorporated in further research, and the viscosity values of normal breast tissue should also be evaluated. Fourth, we did not downgrade BI-RADS categories to maintain the diagnostic sensitivity and specificity of US, however, further researches with large samples were required to validate the rationality of this strategy.

In conclusion, quantitative viscosity-related parameters obtained by US viscosity imaging, especially the Voigt-model-based one, could improve the diagnostic performances of US in characterization of breast lesions with different sizes. Future studies are required to verify this conclusion, and furthermore, to explore the correlation between the viscous property and biological behaviors or prognosis prediction of malignant breast lesions.

DECLARATION OF COMPETING INTEREST

The authors declare that they have no known competing financial interests or personal relationships that could have appeared to influence the work reported in this paper.

APPENDIX A. SUPPORTING INFORMATION

Supplementary data associated with this article can be found in the online version at [doi:10.1016/j.acra.2024.03.017](https://doi.org/10.1016/j.acra.2024.03.017).

REFERENCES

1. Saftoiu A, Gilja OH, Sidhu PS, et al. The EFSUMB guidelines and recommendations for the clinical practice of elastography in non-hepatic applications: update 2018. *Ultraschall Med* 2019; 40:425–453.
2. Mercado CL. BI-RADS update. *Radiol Clin North Am* 2014; 52:481–487.
3. Itoh A, Ueno E, Tohno E, et al. Breast disease: clinical application of US elastography for diagnosis. *Radiology* 2006; 239:341–350.
4. Zhou J, Zhan W, Chang C, et al. Breast lesions: evaluation with shear wave elastography, with special emphasis on the “stiff rim” sign. *Radiology* 2014; 272:63–72.
5. Pillai A, Voruganti T, Barr R, et al. Diagnostic accuracy of shear-wave elastography for breast lesion characterization in women: a systematic review and meta-analysis. *J Am Coll Radiol* 2022; 19:625–634. e620.
6. Berg WA, Cosgrove DO, Dore CJ, et al. Shear-wave elastography improves the specificity of breast US: the BE1 multinational study of 939 masses. *Radiology* 2012; 262:435–449.
7. Bamber J, Cosgrove D, Dietrich CF, et al. EFSUMB guidelines and recommendations on the clinical use of ultrasound elastography. Part 1: basic principles and technology. *Ultraschall Med* 2013; 34:169–184.
8. Kumar V, Denis M, Gregory A, et al. Viscoelastic parameters as discriminators of breast masses: initial human study results. *PLoS One* 2018; 13:e0205717.
9. Manduca A, Bayly PJ, Ehman RL, et al. MR elastography: principles, guidelines, and terminology. *Magn Reson Med* 2021; 85:2377–2390.

10. Shi Y, Qi YF, Lan GY, et al. Three-dimensional MR elastography depicts liver inflammation, fibrosis, and portal hypertension in chronic hepatitis B or C. *Radiology* 2021; 301:154–162.
11. Tapper EB, Loomba R. Noninvasive imaging biomarker assessment of liver fibrosis by elastography in NAFLD. *Nat Rev Gastroenterol Hepatol* 2018; 15:274–282.
12. Patel BK, Samreen N, Zhou Y, et al. MR Elastography of the breast: evolution of technique, case examples, and future directions. *Clin Breast Cancer* 2021; 21:e102–e111.
13. Chen S, Sanchez W, Callstrom MR, et al. Assessment of liver viscoelasticity by using shear waves induced by ultrasound radiation force. *Radiology* 2013; 266:964–970.
14. Zhang XQ, Zheng RQ, Jin JY, et al. US shear-wave elastography dispersion for characterization of chronic liver disease. *Radiology* 2022; 305:597–605.
15. Sugimoto K, Moriyasu F, Oshiro H, et al. The role of multiparametric US of the liver for the evaluation of nonalcoholic steatohepatitis. *Radiology* 2020; 296:532–540.
16. Sugimoto K, Lee DH, Lee JY, et al. Multiparametric US for identifying patients with high-risk NASH: a derivation and validation study. *Radiology* 2021; 301:625–634.
17. Jang JK, Lee ES, Seo JW, et al. Two-dimensional shear-wave elastography and US attenuation imaging for nonalcoholic steatohepatitis diagnosis: a cross-sectional, multicenter study. *Radiology* 2022; 305:118–126.
18. Lee DH, Lee JY, Bae JS, et al. Shear-wave dispersion slope from US shear-wave elastography: detection of allograft damage after liver transplantation. *Radiology* 2019; 293:327–333.
19. Hossain MM, Selzo MR, Hinson RM, et al. Evaluating renal transplant status using viscoelastic response (VisR) ultrasound. *Ultrasound Med Biol* 2018; 44:1573–1584.
20. Barr RG, Zhang Z. Shear-wave elastography of the breast: value of a quality measure and comparison with strain elastography. *Radiology* 2015; 275:45–53.
21. Mann RM, Hooley R, Barr RG, et al. Novel approaches to screening for breast cancer. *Radiology* 2020; 297:266–285.
22. Catheline S, Gennisson JL, Delon G, et al. Measuring of viscoelastic properties of homogeneous soft solid using transient elastography: an inverse problem approach. *J Acoust Soc Am* 2004; 116:3734–3741.
23. American Institute of Ultrasound in M, American Society of Breast S. AIUM practice guideline for the performance of a breast ultrasound examination. *J Ultrasound Med* 2009; 28:105–109.
24. Zhou J, Zhan W, Dong Y, et al. Stiffness of the surrounding tissue of breast lesions evaluated by ultrasound elastography. *Eur Radiol* 2014; 24:1659–1667.
25. Teichgraeber DC, Guirguis MS, Whitman GJ. Breast cancer staging: updates in the AJCC cancer staging manual, 8th edition, and current challenges for radiologists, from the AJR special series on cancer staging. *Am J Roentgenol* 2021; 217:278–290.
26. DeLong ER, DeLong DM, Clarke-Pearson DL. Comparing the areas under two or more correlated receiver operating characteristic curves: a nonparametric approach. *Biometrics* 1988; 44:837–845.
27. Bayat M, Nabavizadeh A, Nayak R, et al. Multi-parameter sub-hertz analysis of viscoelasticity with a quality metric for differentiation of breast masses. *Ultrasound Med Biol* 2020; 46:3393–3403.
28. Sugimoto K, Moriyasu F, Oshiro H, et al. Viscoelasticity measurement in rat livers using shear-wave US elastography. *Ultrasound Med Biol* 2018; 44:2018–2024.
29. Zhang H, Guo Y, Zhou Y, et al. Fluidity and elasticity form a concise set of viscoelastic biomarkers for breast cancer diagnosis based on Kelvin-Voigt fractional derivative modeling. *Biomech Model Mechanobiol* 2020; 19:2163–2177.
30. Coussot C, Kalyanam S, Yapp R, et al. Fractional derivative models for ultrasonic characterization of polymer and breast tissue viscoelasticity. *IEEE Trans Ultrason Ferroelectr Freq Control* 2009; 56:715–726.
31. Sinkus R, Tanter M, Catheline S, et al. Imaging anisotropic and viscous properties of breast tissue by magnetic resonance-elastography. *Magn Reson Med* 2005; 53:372–387.
32. Sridhar M, Insana MF. Ultrasonic measurements of breast viscoelasticity. *Med Phys* 2007; 34:4757–4767.
33. Carmichael B, Babahosseini H, Mahmoodi SN, et al. The fractional viscoelastic response of human breast tissue cells. *Phys Biol* 2015; 12:046001.
34. Park HS, Shin HJ, Shin KC, et al. Comparison of peritumoral stromal tissue stiffness obtained by shear wave elastography between benign and malignant breast lesions. *Acta Radiol* 2018; 59:1168–1175.
35. Evans A, Whelehan P, Thomson K, et al. Invasive breast cancer: relationship between shear-wave elastographic findings and histologic prognostic factors. *Radiology* 2012; 263:673–677.
36. Wang Y, Li Y, Song Y, et al. Comparison of ultrasound and mammography for early diagnosis of breast cancer among Chinese women with suspected breast lesions: a prospective trial. *Thorac Cancer* 2022; 13:3145–3151.